

A Possible 100-day X-ray-to-Optical Lag in the Variations of the Seyfert 1 Nucleus NGC 3516

Dan Maoz¹, Rick Edelson^{2,3,4}, & Kirpal Nandra^{5,6}

ABSTRACT

We present optical broadband (B and R) observations of the Seyfert 1 nucleus NGC 3516, obtained at Wise Observatory from 1997 March to 1998 September, contemporaneously with the X-ray 2–10 keV measurements of *RXTE*. The cross correlation function shows a positive peak when the optical variations lead the X-rays by ~ 100 days, and anticorrelation peaks at various leads and delays between the X-rays and the optical. We show that the putative correlation signal at 100 days is entirely due to the slow ($\gtrsim 30$ days) components of the light curves. During the first year of this monitoring, smoothed versions of the light curves are nearly identical copies of each other, but scaled in amplitude and shifted in time. However, for the next 200 days, the X-ray and optical variations are clearly different. During the whole period, the faster-changing components of the light curves are uncorrelated at any lag.

We consider the detection of these lags tentative and the significance of the correlations uncertain. If the 100-day delay is real, however, one interpretation is that the slowly-varying part of the X-ray emission is an echo of the optical emission, Compton scattered from a medium located at, or extending, $\sim 50 - 100$ light days from the optical source. We point out that a possibly analogous phenomenon, of a lag between hard and soft X-rays for a given variability timescale, exists in Galactic stellar-mass accretors. Remarkably, in both cases the lag corresponds to a light travel distance of order 10^4

¹School of Physics & Astronomy and Wise Observatory, Tel-Aviv University, Tel-Aviv 69978, Israel. dani@wise.tau.ac.il

²Astronomy Department, University of California, Los Angeles, CA 90095-1562

³X-ray Astronomy Group, Leicester University, Leicester LE1 7RH, United Kingdom

⁴Eureka Scientific, 2552 Delmar Ave., Oakland, CA 94602-3017

⁵NASA/Goddard Space Flight Center; Laboratory for High Energy Astrophysics; Code 662; Greenbelt, MD 20771

⁶Universities Space Research Association

gravitational radii. Alternatively, the lag may not represent a physical size, but some other time scale. For example, it may be the manifestation of an instability propagating inward in an accretion flow, appearing first in the optical and then in the X-rays. In any event, we observe no strong correlation at zero lag, or at the small positive lags expected if the optical continuum were produced by reprocessing of X-rays. An energetically-significant reprocessed component in the optical emission of NGC 3516 is thus ruled out by our data.

Subject headings: galaxies: active – galaxies: individual (NGC 3516) – galaxies: Seyfert – x-rays: galaxies

1. Introduction

Much of the energy of Seyfert-1-type active galactic nuclei (AGNs) is emitted in X-rays, yet it is unclear what the source of this emission is. Comparison of variations in different bands can provide valuable clues toward understanding the geometry and nature of AGNs. In particular, inter-band lags can discriminate between primary and secondary (i.e., reprocessed) emissions.

Contemporaneous X-ray and UV/optical monitoring has been carried out for only a few Seyfert 1 galaxies to date. On short time scales, simultaneous optical and X-ray monitoring of both NGC 4051 (Done et al. 1990) and NGC 3516 (Edelson et al. 1999) showed strong X-ray variations and little or no optical changes over 2–3 day periods. Longer time scale monitoring of NGC 5548 (Clavel et al. 1992) and NGC 4151 (Kaspi et al. 1996; Crenshaw et al. 1996; Warwick et al. 1996; Edelson et al. 1996) found evidence for a correlation at zero lag between optical, ultraviolet (*IUE* data), and X-ray (*ROSAT* and *ASCA* data), but these data were very sparsely sampled (≤ 12 points). NGC 7469 was monitored intensively with *RXTE*, *IUE* and ground-based observatories for one month in 1996. The optical and UV were found to be strongly correlated, with evidence presented for a lag that increases with wavelength (Wanders et al. 1997; Collier et al. 1998). There was, however, no clear correlation found between the X-rays and UV (Nandra et al. 1998). The peaks in the X-ray light curve appeared to lag the UV peaks by ~ 4 days, while the troughs appeared better correlated at zero lag. The X-rays also showed much more rapid variations than the UV and, by extension, the optical. Most recently, Chiang et al. (1999) monitored NGC 5548 for three days with *RXTE*, *ASCA*, and the *Extreme Ultraviolet Explorer (EUVE)*. Evidence was presented for a lag that increases with energy band, with the *ASCA* (0.5-1 keV) variations lagging the *EUVE* (0.14–0.18 keV) variations by about 3.5 hours, and the *RXTE* (2–20 keV) variations lagging *EUVE* by about 10 hours.

We initiated in 1997 a program to monitor the Seyfert 1 galaxy NGC 3516 with *RXTE*. Apart from its brightness and known tendency to vary, the high declination of this galaxy makes it circumpolar for most Northern ground-based observatories, allowing it to be observed year round. Month- and year-long variation timescales can thus be properly probed, as well as shorter timescales. Edelson & Nandra (1999) presented the *RXTE* data for NGC 3516 between 1997 March and 1998 September, and calculated the power-density spectrum (PDS) of the 2–10 keV fluctuations on all timescales from 20 min to 6 months. They found that the PDS can be described by a power law of slope -1.7 that turns over to a flatter slope at timescales longer than ~ 1 month.

Here we present densely-sampled optical broad-band (*B* and *R*) measurements of NGC 3516 obtained at Wise Observatory contemporaneously with the *RXTE* monitoring, and supplement the *RXTE* light curve with new data through 1999 January. In §2 we describe the observations and data reduction, and derive the optical light curves. In §3 we carry out a time series analysis comparing the X-ray and optical light curves. In §4 we attempt to interpret our results within a physical picture.

2. Optical Observations and Reductions

We observed NGC 3516 from 1997, March 5, to 1998, September 2, using the Wise Observatory 1m telescope in Mitzpe Ramon, Israel. On the nights when the galaxy was observed, Johnson-Cousins *B*- and *R*-band images were obtained once per night. We used a 1024×1024 -pixel thinned Tektronix CCD at the Cassegrain focus, with a scale of $0.7'' \text{ pixel}^{-1}$. Exposure times were 3 min in *R* and 5 min in *B*. During this 546-day period, useful data were obtained for 108 epochs in *R* and for 87 epochs in *B*. Between 1997 February 1 and November 25 the telescope suffered from scattered-light problems due to a change in baffling. Data from this period could not be properly flat-fielded. However, under proper baffling of scattered light one can see that the detector response and illumination vary by only a few percent across the $12'$ field of view of the detector, so there should only be a minor effect on the accuracy of our photometry. We verify this below.

Aperture photometry was carried out by integrating counts within circular apertures centered on the Seyfert nucleus and on the six brightest unsaturated stars projected near the galaxy. The stars were chosen to be within a few arcminutes from the galaxy, and in various directions, in order to minimize the error due to the lack of proper flatfielding for most of the frames. On some epochs, only the central section of the CCD was read out, and hence not all six comparison stars are present on the frame. Measurements of stars in which any of the pixels were near saturation were discarded. The apertures had a radius

of 4 pixels. For comparison, the seeing half-width at half-maximum (HWHM) was in the range of 1 to 2.5 pixels, with a typical value of 1.5 pixels. The aperture thus included most of the light from a star, even under adverse seeing conditions. The local background level was calculated in annuli of inner and outer radii 8 and 11 pixels, respectively, around each object. For the measurement of the nucleus, this background subtraction provides some removal of the galaxy starlight. We experimented using smaller or larger apertures. We obtained similar light curves for the nucleus, but with smaller variation amplitudes for the larger apertures, due to the larger constant stellar contribution. On the other hand, the errors in the light curves (as determined below) also became larger for small apertures, due to the dependence of the integrated counts on the object-centering accuracy in the pixellated images. We found that the 4-pixel aperture radius was optimal in terms of minimizing both the galaxy background and the photometric errors.

Relative photometry was achieved by calculating the instrumental magnitude difference between a star’s counts in a given epoch and its counts in the first epoch of the program. These differences were averaged among all the comparison stars present on a frame to provide an instrumental zero point for a given epoch. The standard deviation of this mean provided an empirical estimate of the photometric error. The difference of the nuclear instrumental magnitude and the zeropoint of a given epoch yielded the change in magnitude of the nucleus relative to the first epoch. We verified that there is only a barely-discernible effect of the choice of “first epoch” on the final light curves .

To assure that the comparison stars are not variable themselves, and to assess the reliability of our error estimates, we measured in the same way each star using the five other stars as comparisons. We found that the stars are non-variable to within our measurement accuracy. The deviations of a star’s brightness from its mean are consistent with its assigned error-bars, assuming a Gaussian error distribution. The mean error is 0.02 mag. For epochs whose frames contained fewer than four comparison stars, the standard deviation of the zeropoint mean was poorly defined, and the larger among the standard deviation and 0.02 mag was adopted as the error.

Figure 1 shows the optical light curves we have obtained for NGC 3516. In Figure 2 we plot on the same scale for each optical band the constant, to within errors, light curve of one of the comparison stars, calculated relative to the other five stars. The R and B light curves of NGC 3516 in Figure 1 show very similar variability patterns, with peak-to-peak amplitudes of 0.35 mag and 0.7 mag, respectively. There is thus no doubt as to the reality of the variations. As mentioned above, the exact amplitude of the variations depends on the choice of photometric extraction aperture, which will include a particular fraction of stellar light from the galaxy. The above numbers are therefore lower limits on the *intrinsic*

variability amplitude of the nucleus in each band, which is difficult to estimate.

3. Time Series Analysis

Here we compare the X-ray and optical light curves of NGC 3516. All our results apply equally well to both the B and the R light curves, to which we will refer collectively as the “optical light curves”. Since the R light curve is better sampled than the B light curve, we will use only the R in the figures and discussion below. Figure 3 (top panel) shows again the R light curve of NGC 3516, but with a relative linear (rather than magnitude) flux scale. The bottom panel shows the $RXTE$ X-ray (2-10 keV) light curve of Edelson & Nandra (1999), supplemented with new $RXTE$ data up to January 1999. Observations and reduction leading to the new $RXTE$ data are as described in Edelson & Nandra (1999).

Examination of Figure 3 shows that the bulk of the optical variation is in a ~ 250 -day-long rise and fall between days 600 and 850, followed by a two-month-long deep minimum centered around day 1000. The X-ray light curve, by contrast, has much more power in short-timescale flickering.

The z-transformed discrete correlation function (ZDCF; Alexander 1997), a modification of the discrete correlation function (Edelson & Krolik 1988) was used to assess the degree of correlation between variations in the optical and X-ray bands. The top panel of Figure 4 shows the ZDCF for the unsmoothed R -band and X-ray data. A positive correlation of $r = 0.70$ is seen at a lag of $\Delta t \approx -110$ days (that is, with the optical variations leading the X-rays) while an anticorrelation of $r = -0.70$ is found at a lag of $\Delta t \approx -280$ days. Furthermore, anticorrelations of $r = -0.3$ to $r = -0.5$ are seen between lags of $\Delta t \approx +100$ to $+200$ days. We also note that there is a small subpeak close to zero lag.

The significance of the cross-correlation peaks is usually computed using Student’s t-test, with the null-hypothesis probability depending on the number of independent points in the correlation. Usually, this is assumed to be the number of data points in each bin of the ZDCF, and under such an assumption the correlations we find are highly significant. Here we question this assumption, however. It is well-known that the PDSs of AGN, including NGC 3516, have a “red-noise” character, with variations correlated over time scales of ≤ 1 month. The number of *independent* data points in each correlation bin may therefore be greatly reduced, as will the inferred significance of the correlations. The high significance of both the positive and negative correlations also indicates that the underlying assumptions need to be examined. With no straightforward way of estimating the number of independent data points in a given bin, we caution that the significances usually assumed

are almost certainly overestimated.

To obtain a more quantitative assessment of the significance of the correlation, we have carried out Monte Carlo simulations, as follows. Synthetic light curves having chosen PDSs were created by summing suitably-weighted harmonic functions with random phases. The synthetic light curves were then sampled with the same temporal pattern as the real optical and X-ray light curves. Simulated Gaussian measurement errors were added as each point, such that the ratio of the rms variation of the light curve to the Gaussian σ was typical of that of the real light curves. The cross-correlation function of the simulated optical and X-ray light curves was then searched for values as high as the one observed in the real data. The whole process was repeated 1000 times for each choice of optical and X-ray PDS, and the fraction of iterations with correlation above the threshold noted.

We find the results of these simulations are strongly dependent on the assumed PDS of each light curve. Edelson & Nandra (1999) showed that the X-ray PDS of NGC 3516, on timescales shorter than about 1 day, is well described by a power law of index $\alpha_x = -1.74 \pm 0.12$. On longer timescales, however, the index gradually flattens, to $\alpha_x \approx -1.0$ on day-long to month-long timescales, and further to $\alpha_x \approx -0.7$ on few-month timescales. The PDS slope on timescales longer than one day, precisely the timescales probed here, is not well constrained. The observational knowledge of the optical PDS is much worse. The uneven sampling of the optical light curve precludes any straightforward calculation of its PDS. Existing algorithms, e.g. Scargle (1982), for calculating the PDS of unevenly sampled data, are useful for periodicity searches, but badly fail to reproduce the shape of PDS's having power over a broad range of frequencies, due to the aliasing between frequencies that the uneven window function introduces. (See Giveon et al. 1999, for a detailed discussion of the problem.) To obtain a very rough guide of the optical PDS shape, we applied to the data Giveon et al.'s (1999) "partial interpolation" algorithm. The results suggest the optical PDS may be a power law of slope $\alpha_o \sim -2.0 \pm 0.6$.

Given the above uncertainties with regard to the PDS's that must be input to the simulations, we calculated the significance of the observed correlation for a grid of power-law PDS's with different slopes. The significance of the correlation is highest for flat input PDS slopes, and becomes low for steep PDS's, in which each light curve is dominated by only a few "events" which can produce spurious correlations. For an input X-ray PDS slope of $\alpha_x = -1.0$, which is a reasonable choice, the observed correlation is significant at $> 99\%$ confidence, as long as the optical PDS slope $\alpha_o \geq -1.5$. For $\alpha_o = -1.75$ the significance declines to 98.5%, and for $\alpha_o = -2.5$ it is only 97%. Steeper optical PDS's are allowed for α_x somewhat flatter than -1.0 , and vice versa. We conclude that the observed X-ray-to-optical correlation at 110-day lag may indeed be significant, but the

verdict depends on poorly known parameters. We also note that, as shown below, the observed correlation is actually driven only by the first year’s worth of data, during which the correlation is much higher. However, calculating the significance of only a segment of the data obtained would involve *a posteriori* statistics, which is something we will avoid.

To study the relative contributions to the correlations made by fast and slow variations, we have smoothed the light curves with a 30-day boxcar running mean, and recalculated the ZDCF. The smoothed light curves are shown as solid lines in Figure 3. The middle panel of Figure 4 shows the ZDCF for the smoothed data, and the bottom panel, the ZDCF for the residuals (i.e., the original light curves minus their respective smoothed versions). The smoothed light curves show correlations and anticorrelations that are similar, but somewhat strengthened, compared to the unsmoothed light curves, with a positive peak of $r = 0.80$ at $\Delta t = -100$ days, a negative peak of $r = -0.90$ at $\Delta t = -280$ days, and a negative plateau of $r \approx -0.65$ at $\Delta t = +100$ to $+200$ days. The correlation function of the residual light curves shows no significant signal, indicating that there is no correlation present in the high temporal frequency components of the data.

We obtain similar results if, instead of using the ZDCF algorithm, we use a “least-squares shift and scale” scheme to find the best lag for the observed, smoothed, or residual light curves. For every time-shift between the light curves, we find the linear relation that, when applied to the X-ray light curve, minimizes the sum of the square of the differences between each optical point and the scaled X-ray point that is nearest in time to it at that shift. The global (over all time shifts) least squares then provides the best lag.

On the face of it, the positive peak in the correlation suggests that the optical variations lead the X-ray variations by ~ 100 d. The similarity between the smoothed optical and X-ray light curves during the first 350 days can be seen in Figure 5, which shows the two after the X-rays are scaled, and shifted back in time, according to the least-squares solution for this period. This figure clarifies the fact that the strong apparent correlation we observe is driven primarily by one “event” in the light curve. Indeed, one sees a complete mismatch, at this lag, of the light curves after day 850. The deep minimum observed in the optical light curve seems to correspond at zero lag to a local minimum in the X-ray light curve, which may account for the subpeak in the ZDCF at zero lag. This increases the likelihood that we are perhaps being misled by chance similarities in temporal structure of parts of the light curves, while in fact there is no correlation between the variations in the different bands. Also, the anti-correlations mentioned above have similar significance to that of the positive peak, and while there have been no physical mechanisms proposed to explain an anticorrelation between the bands, there is no statistical reason to prefer positive correlations over negative ones. Continued monitoring may help discriminate between these

options, whose physical implications we discuss in the next section.

We have also cross-correlated the optical light curves themselves. The ZDCF of the B vs. R light curves (Figure 6) shows, as expected, that they are highly correlated ($r = 0.95$), but the peak and the centroid of the ZDCF are slightly shifted from zero lag, indicating the R variations lag the B variations by several days (which is comparable to the mean sampling interval). While this delay could be interpreted as a wavelength-dependent continuum lag, we believe a more likely explanation is the fact that the strong broad $H\alpha$ line is included in the R band, and contributes of the order of 10-20% of the broad-band flux. Balmer-line variations in this galaxy lag the continuum variations by about 11 days (Wanders et al. 1993) due to the light-travel time across the broad-line region. The $H\alpha$ contribution to the R band probably shifts slightly the ZDCF peak from the peak at or near zero lag that it would have if there were only variable continuum emission in the band. The observed delay may therefore be considered an upper limit on the true delay between B and R .

4. Discussion

Much current thinking about the emission processes in AGNs centers around the notion that the X-rays arise from very close (within a few Schwarzschild radii, R_S) of a massive black hole. Support for this idea has come from the rapid variability that is observed in X-rays (implying small physical scales), as well as the detection in X-rays of a broad Fe K-shell emission line in many Seyfert 1s (e.g. Nandra et al. 1997). The emission line is thought to be gravitationally and Doppler broadened fluorescence of the inner parts of an accretion disk, after the disk is illuminated by the X-rays. The continuum-emission mechanism is not known, but most commonly it is assumed that the X-rays are optical/UV photons which have been upscattered by a population of hot electrons. The acceleration mechanism and geometry of the X-ray source is not known. Neither is the source of seed photons, and despite some substantial problems it is still usually assumed that the optical/UV arises directly from an accretion disk (Shields 1978; Malkan 1983). It has also been hypothesized that X-rays illuminating the disk, or other optically thick gas, might be responsible for some or all of the optical/UV radiation, via reprocessing (Guilbert & Rees 1988; Clavel et al. 1992).

Variability data such as those we have presented above can provide stringent constraints on possible models. In summary, our data have shown strong variability in both optical and X-ray bands on month-to-year time scales, but rapid (days) variations only in the X-rays. The zero-lag correlation between the bands is poor, with a much stronger relationship implied if the optical variations lead those in the X-rays by $\sim 100d$. This “100-day lead”

breaks down in the latter parts of the monitoring period. Strong negative correlations are also observed for optical leads of 280 d and optical *lags* of 100 – 200d. This makes us cautious about the reality of the lag, but we will discuss some physical implications of our results below.

It has long been suspected that the X-rays show more rapid variations than the optical/UV, and this has been explicitly demonstrated in a few cases (e.g., NGC 4051, Done et al. 1990; NGC 7469, Nandra et al. 1998; NGC 3516, in a 3-day HST/RXTE/ASCA campaign, Edelson et al. 1999). Our data add to that body of evidence, which implies, unavoidably, either that the observed optical radiation is not the primary seed photon source, or that the process which turns these photons into X-rays induces variability intrinsically. Given a supposed location in the inner few R_S , it might be more natural to assume that UV or EUV photons are the seeds for the X-rays. With an origin in the inner disk, the EUV emission would be expected to be more variable, although it is still extremely difficult to reconcile variability as rapid as that observed with physical time scales in the disk (Molendi, Maraschi & Stella 1992). The X-ray source itself may be less directly connected to the disk physics, and could, in principle, change much more rapidly, especially if consisting of multiple flaring regions, as opposed to a single, coherent one.

We have also shown tentatively that the X-rays may respond on long ($\sim 100d$) time scales to variations in the optical. One way of viewing the 2–10 keV emission, then, is as the sum of two components: a smoothly-varying component that is very similar to the optical light curves during the first year, but lags them by ~ 100 days, and a fast, flickering, component that is uncorrelated with the optical variations. The seeming lack of a deep minimum in the X-ray light curve, corresponding to a delayed version of the minimum seen in the optical light curve around day 1000, could arise because the slow, delayed component had nearly turned off, and the X-ray emission had become dominated by the second component. Indeed, if a constant is subtracted from the smoothed X-ray light curve, such that the smoothed curve always passes below the observed X-ray measurements (to ensure that the flux in the fast component is always positive), then the lowest points in the smoothed light curve just reach zero flux (see Figure 3). The delay of the smooth component behind the optical emission could then be interpreted as the light-travel time between the seed photon source and a Compton upscattering region. If it is not the optical photons themselves being upscattered, we would need to assume that the variations of the optical light curves can serve as surrogates for some other seed photon (UV or soft X-ray) variations. The large delay observed would put the scatterer at a relatively large distance, $r \approx 50 - 100$ lt-days ($1.25 - 2.5 \times 10^{17}$ cm) from the nucleus, i.e. $\sim 10^4 R_S$ (for a $10^8 M_\odot$ black hole).

It is possible to imagine a toy model of the required “Compton mirror” by surrounding the nucleus with a $T \approx 3 \times 10^9 K$ (or hotter, depending on the energy of the seed photons) electron gas in a thin ($\Delta r \lesssim 20$ lt-days = 5×10^{16} cm) 50-lt-day-radius shell of density $n \approx 2 \times 10^6 \text{ cm}^{-3}$ and column density $N \approx 10^{23} \text{ cm}^{-2}$, giving a low optical depth to Compton scattering of $\tau \sim 0.1$. The geometrical thinness is constrained by the small amount of broadening allowed by the data between the X-ray and optical pulse. This configuration would ensure that only photons that are singly backscattered by large angles are upscattered to the 2-10 keV band, so that a coherent echo is seen only from a small cap on the far side of the shell. This optical depth will also roughly produce the observed ratio of 1 keV and 3 keV photons in this object, corresponding to the photon index $\Gamma \approx 2$ between 0.6–10 keV measured by George et al. (1998). However, more sophisticated calculations are required to see if the observed variations and detailed spectrum can be reproduced in this scenario. As already mentioned, this picture also leaves the rapid variability of the X-rays unexplained, so we must then invoke either another X-ray producing-region closer to the black hole, or an extended region, which produces emission at various radii (and therefore variations with a range of time scales).

Similar models have been proposed to explain the emission in Galactic stellar-mass accreting neutron stars and black holes. For individual bins of frequencies in the X-ray Fourier spectrum of such objects, the hard X-rays lag the soft X-rays by an approximately-constant phase, meaning there is a time lag that increases linearly with the Fourier timescale probed. For low frequencies (0.1 Hz) the time lag is about 0.2 s, corresponding, again, to $10^4 R_S/c$ (e.g., van der Klis et al. 1987; Miyamoto et al. 1992; Vaughan et al. 1994; Ford et al. 1999). Here, too, it has been proposed that the lags are due to light-travel time in a very extended Compton upscattering gas (e.g., Sunyaev & Truemper 1979; Payne 1980; Kazanas, Hua, & Titarchuk 1997; Hua, Kazanas & Cui 1999). The more recent of these models invoke a centrally-concentrated distribution of gas, although the similarity of the optical and X-ray light curves in NGC 3516 are suggestive of the thinner shell referred to above.

This picture is not free of problems. A separation into two (or more) X-ray components may be considered *ad hoc*. There are also strong implications from the spectral observations that the bulk of the X-ray continuum is concentrated in the central regions, arguing against a region extending to many thousand gravitational radii. We have not considered how the Compton-upscattering gas is heated to its high temperature at such a large radius. A similar problem is encountered for the X-ray binaries (e.g. Stollman et al. 1987). Solutions that have been suggested include that, for black holes, the gas is heated locally as part of an advection dominated accretion flow (ADAF, e.g. Narayan & Yi 1994), or, for neutron stars, that the gas was preheated by radiation from the central source (Kazanas et al. 1997), or

that the energy is transported via magnetic fields (Stone et al. 1996).

Alternatively, the 100d signal may be associated not with a light-travel time, but with some other time scale. One interpretation that is more in line with standard thinking about the inner regions of AGNs is that we are witnessing the effects of an inhomogeneous accretion flow onto the black hole. The time inferred from the optical-X-ray lag is then some timescale associated with the disk, or accretion, process. Some form of instability, e.g., thermal or viscous, forms in the disk and causes its optical emission to brighten. The instability then propagates inwards to the hotter, X-ray emitting radii, on a timescale of 100 days, when an X-ray “copy” of it is seen in the light curve. One problem with this scenario, however, is that it is unclear why the shapes of the variability patterns would be so similar in the two bands during the first year, implying that the instability spent very nearly equal time intervals in the optically-emitting and X-ray-emitting regions. The lack of correlation in the latter parts of the observation is also unexplained, meaning that the processes in the inner disk are far more complex than what we have just described.

These kind of explanations have also been put forward for the hard X-ray lags in Galactic accretors. For example, Orosz et al. (1997) found that the optical brightening of the “microquasar” GRO-J1655-40 preceded its X-ray (2-12 keV) outburst by 6 days, and suggested this was the result of an inward propagation of a disturbance in the accretion disk. Bottcher & Liang (1999) also presented models for accretion of a cool blob in an advection dominated flow, with the blob’s radiation being Compton upscattered by a progressively hotter and denser corona as it drifts toward the event horizon at constant radial velocity. Alternatively, Poutanen & Fabian (1999) suggest that the lags reflect the timescale for development of a magnetic flare that floats out of a thin accretion disk into a hot, optically-thin, corona, emitting progressively harder radiation until the flare ends suddenly. Applied to AGNs, their model has the attraction of naturally maintaining consistency with the fast variability time scales in the X-ray, as well as the strength and extreme broadening of the iron $K\alpha$ line. These pose serious problems for both the extended-corona and the ADAF models.

We must also keep in mind the possibility that the similarity of the X-ray and optical light curves at 100-days lag during the first year of our program may just be a chance coincidence, and that this is the reason for the extreme differences between the light curves after the first year. Even if there is no real correlation between the variability in these different bands, our data still constrain the origin of the optical emission. We observe no strong correlation at zero lag, or at the small positive lags expected if the optical continuum were produced by reprocessing of X-rays. An energetically-significant reprocessed component in the optical emission of NGC 3516 is ruled out by our data (c.f.

NGC 7469, Nandra et al. 1998).

Interpretation aside, we also note that both the 100-day lag between X-rays and optical, and the 30-day timescale that separates the slow, possibly-correlated X-ray variations from the fast, uncorrelated X-ray flickering, are similar to the turnover timescale in the PDS found for this object by Edelson & Nandra (1999). It will be interesting in the future to construct more specific models which can tie together these time scales.

We would like to thank the following observers at Wise, who contributed their efforts and observing time to obtain the data presented here: R. Be’eri, T. Contini, J. Dann, A. Gal-Yam, U. Giveon, A. Heller, S. Kaspi, Y. Lipkin, I. Maor, H. Mendelson, E. Ofek, A. Retter, O. Shemmer, G. Raviv, and S. Steindling. We are also grateful for the assistance of the Wise Observatory staff: S. Ben-Guigui, P. Ibbetson, and E. Mashal. We acknowledge valuable discussions with N. Arav, I. George, A. Laor, A. Levinson, H. Netzer, A. Sternberg, and J. Turner. T. Alexander is thanked for providing his ZDCF code, and the anonymous referee for useful suggestions. Multiwavelength studies at Wise Observatory are supported by a grant from the Israel Science Foundation.

REFERENCES

- Alexander, T. 1997, in “Astronomical Time Series”, eds. D. Maoz, A. Sternberg, and E.M. Leibowitz (Dordrecht: Kluwer), 163
- Bottcher, M., & Liang, E.P. 1999, *ApJL*, in press
- Chiang, J., et al. 1999, *ApJ*, submitted
- Clavel, J., et al. 1992, *ApJ*, 393, 113
- Collier, S.J. et al. 1998, *ApJ*, 500, 162
- Crenshaw, D.M. et al. 1996, *ApJ*, 470, 322
- Done, C. et al. 1990, *MNRAS*, 243, 713
- Edelson, R.A., & Krolik, J.H. 1988, *ApJ*, 333, 646
- Edelson, R.A., et al. 1996, *ApJ*, 470, 364
- Edelson, R., & Nandra, K. 1999, *ApJ*, 514, 682
- Edelson, R. et al. 1999, in preparation
- Ford, E.C., van der Klis, M., Mendez, M., van Paradijs, J., & Kaaret, P. 1999, *ApJ*, 512, L31

- George, I., Turner, T.J., Netzer, H., Nandra, K., Mushotzky, R., Yaqoob, T. 1998, ApJS, 114, 73
- Giveon, U., Maoz, D., Kaspi, S., Netzer, H., & Smith, P.S. 1999, MNRAS, 306, 637
- Guilbert, P.W., & Rees, M.J. 1988, MNRAS, 233, 475
- Kaspi, S., et al. 1996, ApJ, 470, 336
- Kazanas, D., Hua, X.-M. & Titarchuk, L. 1997, ApJ, 480, 735
- Malkan, M.A. 1983, ApJ, 268, 582
- Miyamoto, S., et al. 1992, Ap, 391, L21
- Molendi, S., Maraschi, L., & Stella, L. 1992, MNRAS, 255, 27
- Nandra, K., George, I.M., Mushotzky, R.F., Turner, T.J., & Yaqoob, T. 1997, ApJ, 477, 602
- Nandra K., et al. 1998, ApJ, 505, 594
- Narayan, R. & Yi, I. 1994, ApJ, 428, L13
- Orosz, J.A., Remillard, R.A., Bailyn, C.D., & McClintock, J.E. 1997, ApJ, 478, L83
- Payne, D.G. 1980, ApJ, 237, 951
- Poutanen, J. & Fabian, A.C. 1999, MNRAS, 306, L31
- Scargle, J.D. 1982, ApJ, 263, 835
- Shields, G.A. 1978, Nature, 272, 706
- Stollman, G.M. et al. 1987, MNRAS, 227, 7P
- Stone, J.M., Hawley, J.F., Gammie, C.F., & Balbus, S.A. 1996, ApJ, 463, 656
- Sunyaev, R.A., & Truemper, J. 1979, Nature, 279, 506
- van der Klis, M., et al. 1987, ApJ, 319, L13
- Vaughan, B., et al. 1994, ApJ, 421, 738
- Wanders, I., et al. 1993, A&A, 269, 39
- Wanders, I., et al. 1997, ApJS, 113, 69
- Wang, J.X., Zhou, Y.Y., Xu, H.G., and Wang, T.G 1999, ApJ, 516, L65
- Warwick, R.S., et al. 1996, ApJ, 470, 349

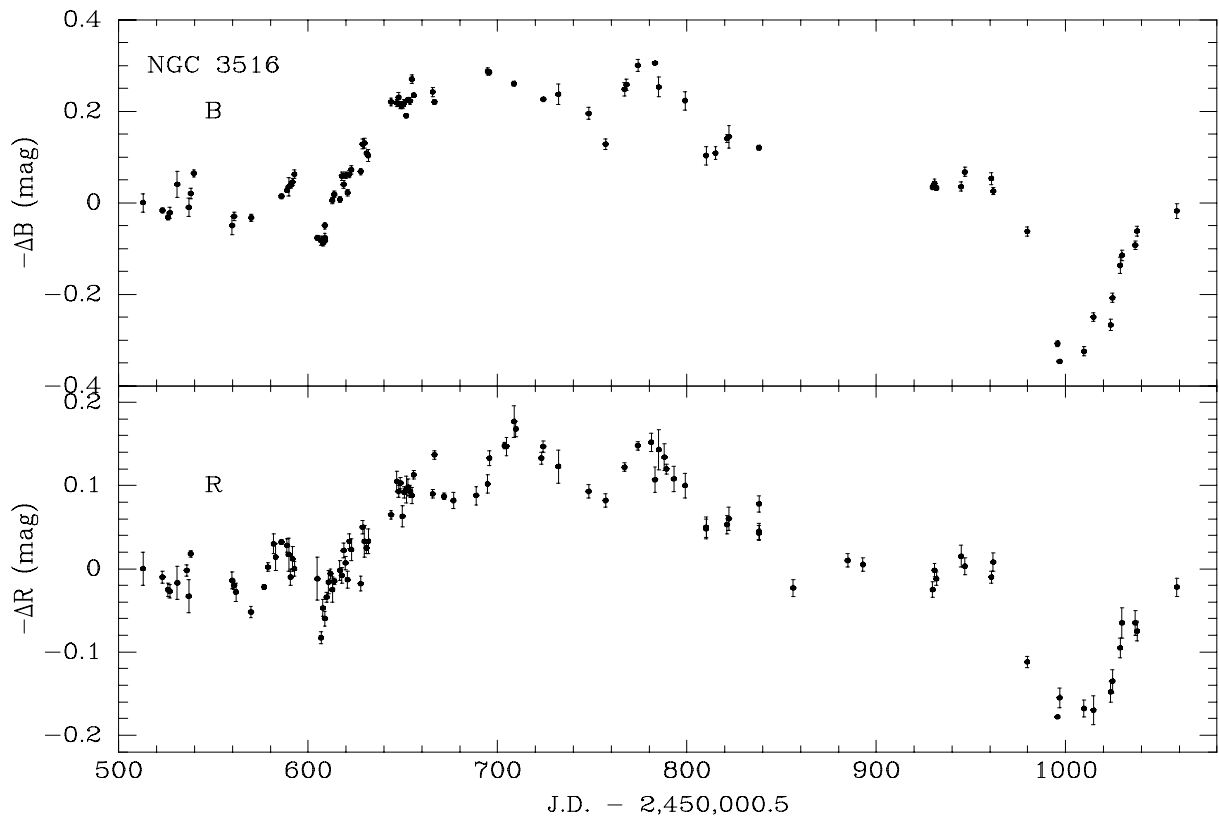


Fig. 1.— *B*-band (top panel) and *R*-band (bottom panel) light curves for NGC 3516.

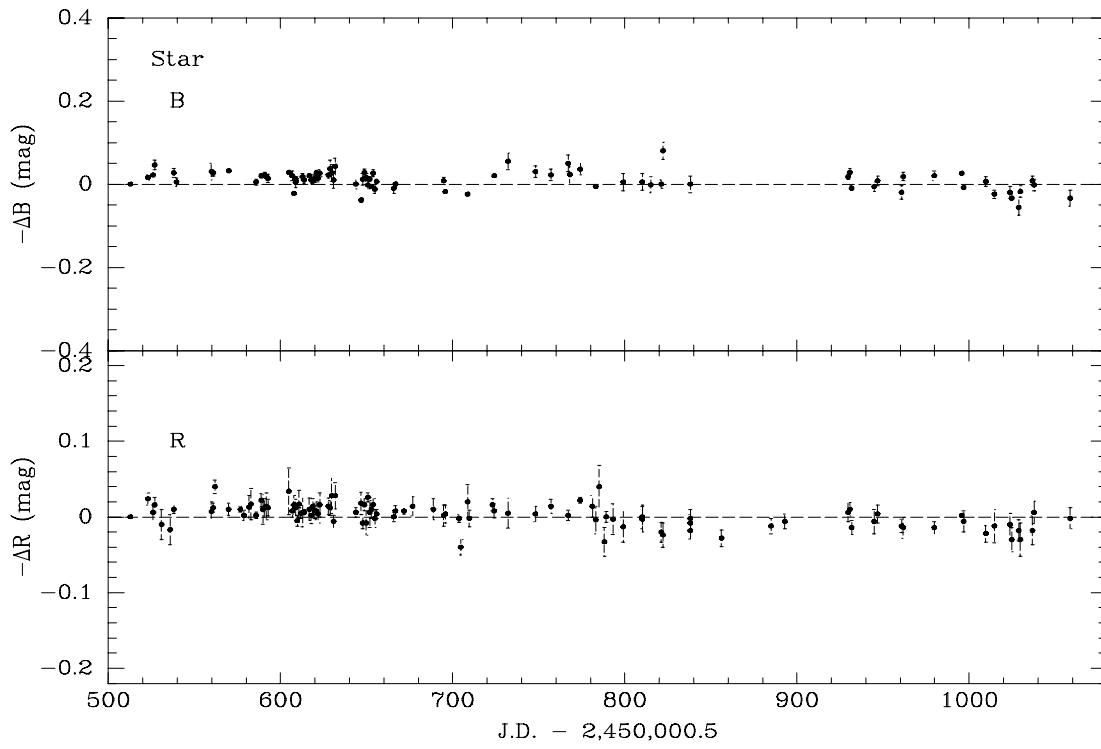


Fig. 2.— *B*-band (top panel) and *R*-band (bottom panel) light curves for one of the comparison stars, measured in the same way as the Seyfert nucleus.

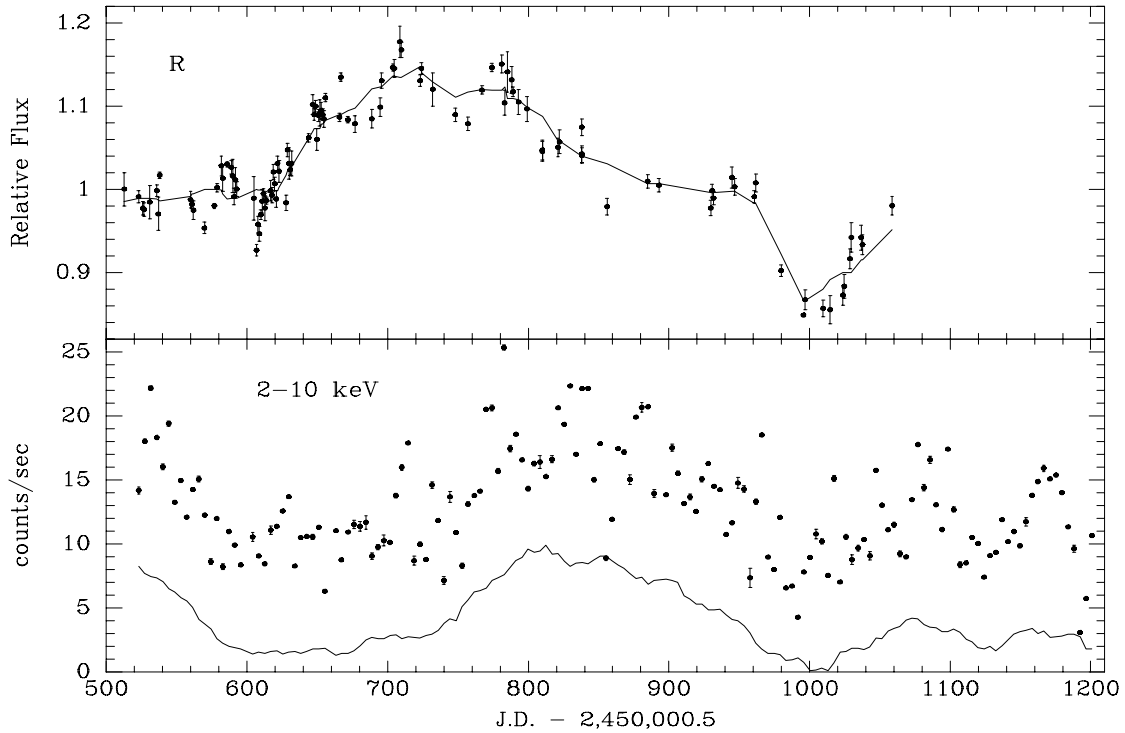


Fig. 3.— Top panel: R -band light curve of NGC 3516, but with linear flux scale. Solid line is 30-day boxcar smoothed version of the light curve. Bottom panel: $RXTE$ X-ray (2-10 keV) light curve of Edelson & Nandra (1998), supplemented with new $RXTE$ data up to January 1999. Solid line is a 30-day smoothed version of the X-ray light curve, vertically shifted so as to lie below all the X-ray measurements.

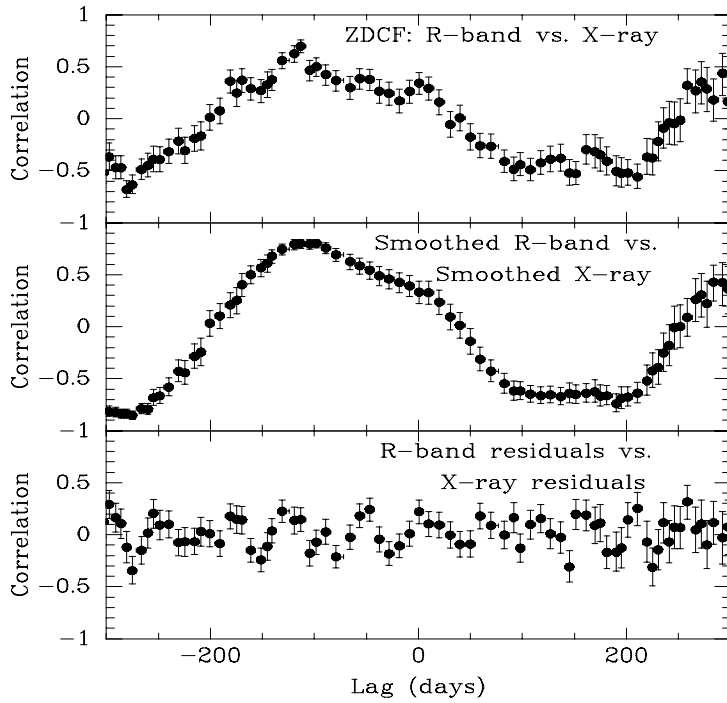


Fig. 4.— ZDCF cross-correlations. Top panel: R -band vs. X-ray light curves. Middle panel: Same as above, but after the light curves have been smoothed with a 30-day boxcar running mean (see Fig. 3). Bottom panel: As above, but between the fast components of the X-ray and R -band light curves, which are obtained by subtracting from each light curve its smoothed version.

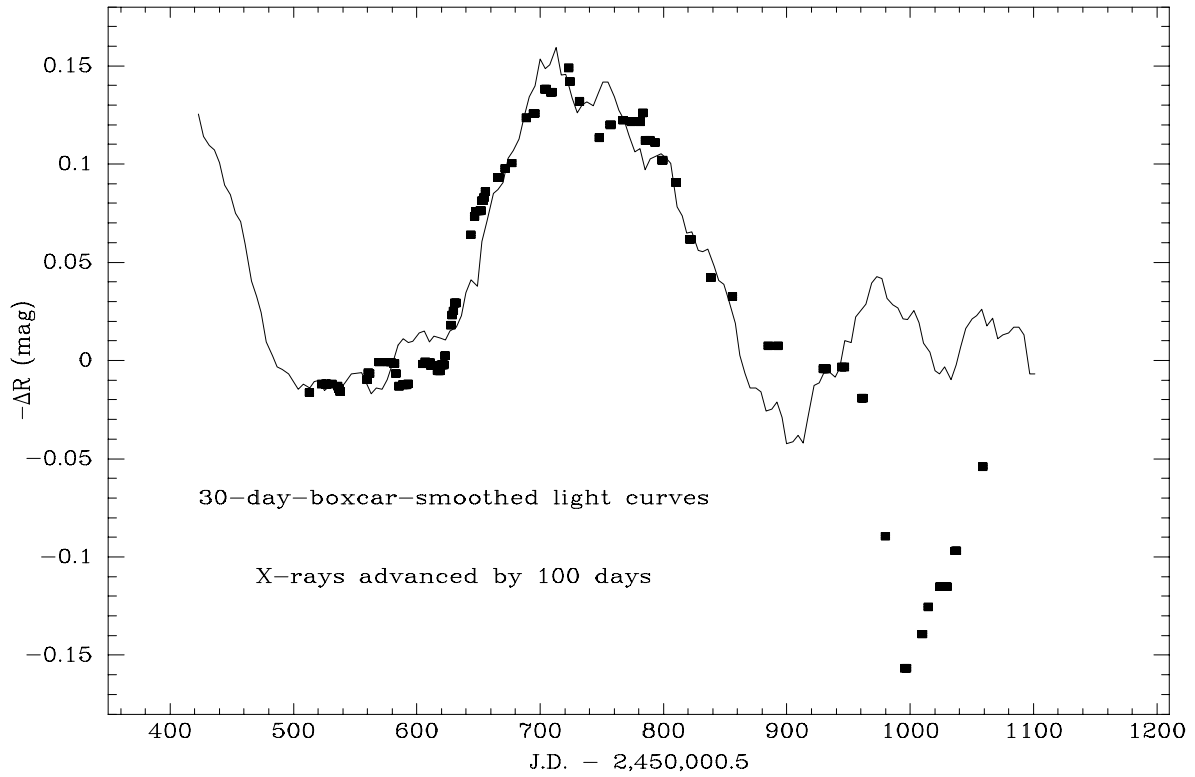


Fig. 5.— Smoothed R -band light curve (boxes), and smoothed X-ray light curve (solid line) after the latter was advanced by 100 days and scaled linearly to obtain the best match between the two during the first year of data. Note the similarity of the two smoothed light curves during the first year, and the dissimilarity thereafter.

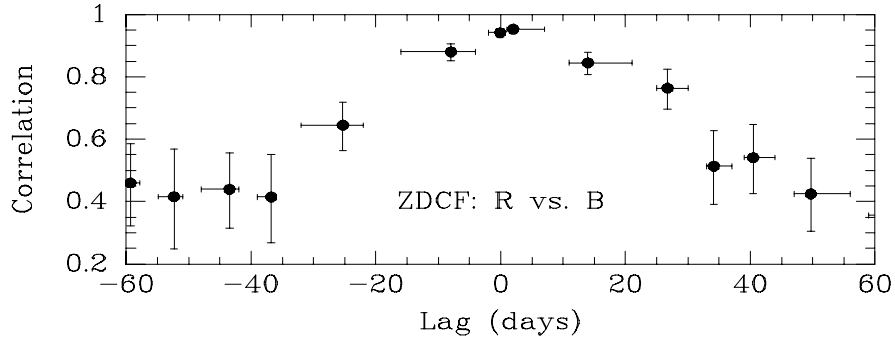


Fig. 6.— ZDCF cross-correlation between the *B* and *R* optical light curves. The small lag of *R* behind *B* which is implied is likely due to the broad $H\alpha$ contribution to the *R* band.